

# Oldhamite: a hidden key mineral for C-O-S-Ca cycles in Earth

Yuegao Liu<sup>1†</sup>, I-Ming Chou<sup>1</sup>, Jiangzhi Chen<sup>1‡</sup>, Oliver Tschauner<sup>2</sup>, Nanping Wu<sup>1</sup>,  
Wenyuan Li<sup>3</sup>, Leon Bagas<sup>3</sup>, Minghua Ren<sup>2</sup>, Shenghua Mei<sup>1\*</sup>, Liping Wang<sup>4\*</sup>

<sup>1</sup>CAS Key Laboratory for Experimental Study under Deep-sea Extreme Conditions, Institute of Deep-sea Science and Engineering, Chinese Academy of Sciences; No. 28 Luhuitou Road, Sanya 572000, Hainan, P.R. China.

<sup>2</sup>Department of Geoscience, University of Nevada, Las Vegas; 4505 S. Maryland Pkwy, Las Vegas, NV 89154, United States.

<sup>3</sup>Xi'an Center of Geological Survey, China Geological Survey; No. 438 Youyi Road, Xi'an 710054, Shaanxi, P.R. China.

<sup>4</sup>Academy for Advanced Interdisciplinary Studies, Southern University of Science and Technology; No. 1088, Xueyuan Avenue, Shenzhen 518055, Guangdong, P.R. China.

\*Corresponding author. Email: [mei@idsse.ac.cn](mailto:mei@idsse.ac.cn) (S.H.M);  
[wanglp3@sustech.edu.cn](mailto:wanglp3@sustech.edu.cn) (L.P.W)

†‡ These authors contributed equally to this work.

## Abstract

**In the solar system, oldhamite (CaS) is present under highly reducing conditions, such as in enstatite chondrites and at the Mercury's surface. Oldhamite is barely observed on Earth because of the combined effects of high abundance of water and oxidizing conditions. Here we show the formation of oldhamite through reaction between sulfide-bearing high-Mg basaltic melts and molten CaCO<sub>3</sub> at 1.5 GPa/1510 K and 0.5 GPa/1320 K with oxygen fugacities below FMQ–0.52 (FMQ = fayalite-magnetite-quartz buffer, in lgf<sub>O2</sub>). Our result indicates that oldhamite can form in the interior of Earth and terrestrial planets with active**

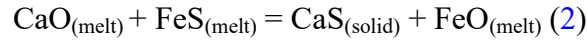
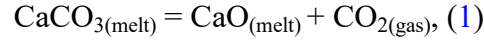
**volcanism. Oldhamite is a plausible precursor for the magmatic sulfate minerals in the mid-ocean ridges.**

After he discovered the elemental alkaline- and alkaline earth elements, Humphrey Davy had proposed that the violent reactions of alkaline metals with oxygen or water are the driving force of terrestrial volcanism (1). This hypothesis was soon abandoned although we know that water plays an important role in arc volcanism and mantle-metasomatism. Alkaline- and alkaline-earth sulfides such as oldhamite are extremely rare in terrestrial igneous rocks. To date, only two studies report the suspected discovery of oldhamite in natural terrestrial rocks. One is in volcanic glass from the Arteni massif (2), and the other is from an impactite (3). However, oldhamite (CaS) is potentially abundant on Mercury's surface (4), and it is a common mineral in enstatite chondrites (5). In both cases the highly reducing conditions with an oxygen fugacity well below IW-2.7 (IW = iron-wüstite redox buffer, in  $\lg f_{\text{O}_2}$ ) stabilize oldhamite (6). It has been proposed that CaS may form by condensation in the solar nebula (7) or through igneous processes in meteorite parent bodies (8).

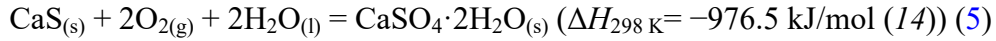
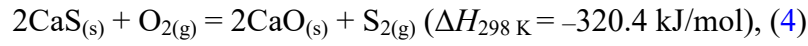
Here we show that oldhamite forms under conditions compatible with the Earth's upper mantle through the reaction between sulfide-bearing orthopyroxenite and  $\text{CaCO}_3$  at 1.5 GPa/1510 K and 0.5 GPa/1320 K in a graphite-lined  $\text{Au}_{75}\text{Pd}_{25}$  capsule (Fig. S3). Oldhamite was observed in the central reaction zone of recovered samples (Figs. S3 and S4). Hereafter we refer to this formation process as the

sulfide-magma-calcite (SMC) interaction. In the absence of  $\text{CaCO}_3$ , experiments under otherwise identical conditions produce partial melt from orthopyroxenite are similar in composition. In both cases the melts are high-Mg basaltic magmas (with  $\text{SiO}_2 = 54.5\text{--}54.9$  wt%,  $\text{MgO} = 9.54\text{--}10.19$  wt%; [Supplementary text section and Table S3](#)). This is consistent with the partial melting process of mantle pyroxenites that in part produced mid-ocean ridge basalts (MORBs) and Hawaiian shield basalts (9, 10). It is worth noting that similar high-Mg basaltic melt is the parent magma of some magmatic Cu-Ni-Pt deposits, which is derived from the mantle but usually interacted with crustal carbonate (11). The oxygen fugacity in the graphite-lined noble metal capsule used in this study is about FMQ-2.2 (12) (FMQ = fayalite-magnetite-quartz redox buffer, in  $\lg f_{\text{O}_2}$ ). Hence, our experiments simulate the reaction between basaltic and carbonate magma in the mantle and the reaction process between basaltic magma and crustal carbonate. Based on our findings ([Figs. S3, S4](#)), oldhamite exists in the mantle under these conditions. However, this point requires a closer look on the redox conditions and energetics of decomposition reactions of oldhamite in the mantle. We compare the paragenesis of oldhamite in meteorites with our run products. In the former, kernels of portlandite,  $\text{Ca}(\text{OH})_2$ , are surrounded by concentric growth of oldhamite,  $\text{CaS}$ , as intermediate, and by pentlandite,  $(\text{Fe,Ni})_9\text{S}_8$ , as an outer zone (13). This paragenesis is interpreted as a result of thermal decomposition of  $\text{CaCO}_3$  into  $\text{CaO}$ , which subsequently reacted with sulfide to form oldhamite (13). In our run products, pentlandite or pyrrhotite are present around

oldhamite, and cavities formed by bubbles are always present close to oldhamite (Figs. S3 and S4). Hence, the most probable route for CaS formation is:



In natural terrestrial samples, the occurrence of CaS is generally constrained by the following reactions



As seen from these equations, CaS can be easily oxidized to form CaSO<sub>4</sub> or CaSO<sub>4</sub>·2H<sub>2</sub>O. The oxygen fugacity at the oldhamite-anhydrite equilibrium (Equation 3, named the OA buffer) and the oldhamite-lime-sulfur equilibrium (Equation 4, named the OLS buffer) can be determined by Equations 6 and 7, respectively (also refer to Supplementary text section):

$$\lg f_{\text{O}_2} = 2.19144 + 1.09305 \times 10^{-4} T - 25137/T - 1551.42/T^2 + 1.5305 \times 10^7/T^3 + 0.04777P/T + 2.7838 \lg T, \quad (6)$$

$$\lg f_{\text{O}_2} = -21.1162 + 3.65342 \times 10^7/T^3 - 6205.07/T^2 + (-16237.94 - 0.11450P)/T + 0.43722 \times 10^{-3} T + 11.13544 \lg T + \lg f_{\text{S}_2} \quad (7)$$

where  $P$  is pressure in bar, and  $T$  is temperature in K. The results are summarized in Figure 1.

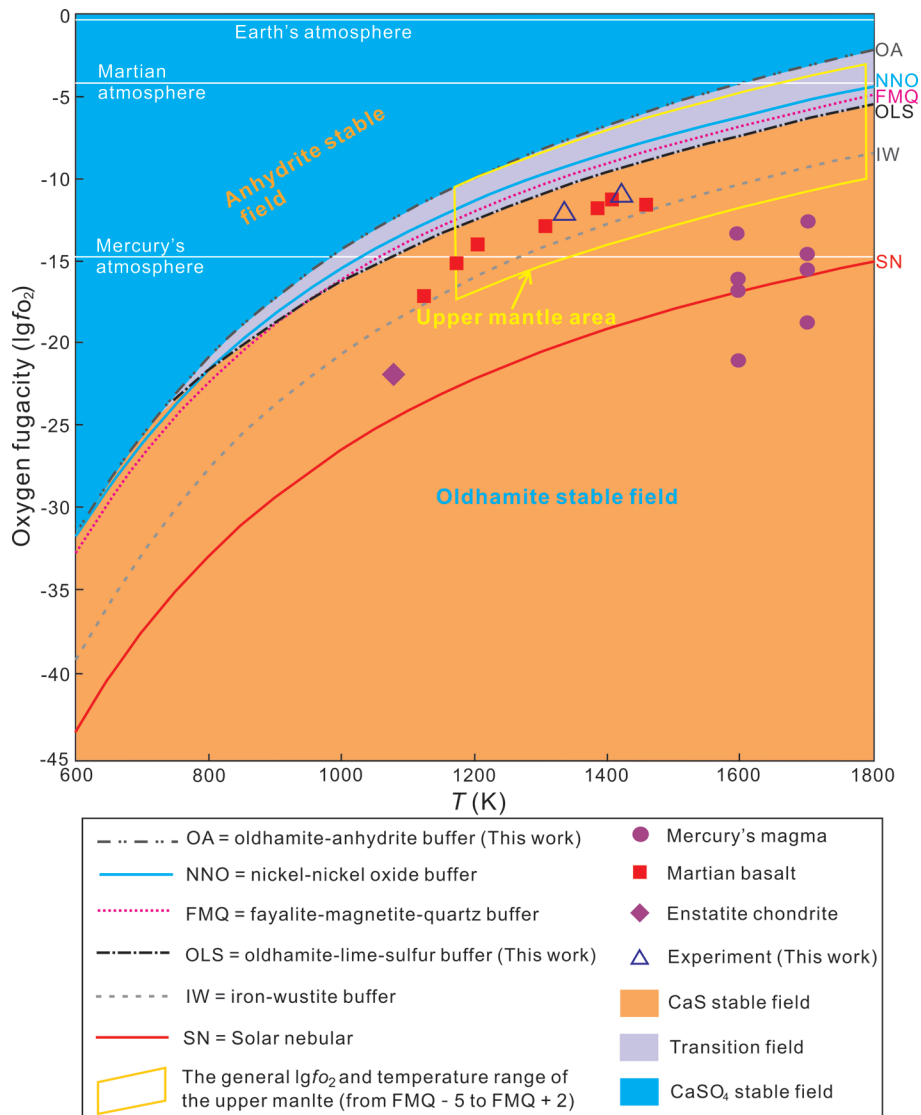


**Fig. 1.** Representative oxygen fugacity buffer at 0.5 GPa total pressure vs. temperature curves and the distributions of some natural and experimental samples. References: NNO is from Ref. (15), and FMQ and IW are from Ref. (16);  $\lg f_{S_2}$  value of  $-12$  (mean sulfur fugacity of black smoker (17)) was used during the OLS calculation. Values of solar nebula  $\lg f_{O_2}$  are calculated from the equation  $\lg f_{O_2} = -0.85 - 25,664/T$ , where  $T$  is in K (18). The  $\lg f_{O_2}$  values of enstatite chondrite, Martian basalt, and the silicate melts on the Mercury's surface are from Ref. (6), Ref. (19), and Ref. (20), respectively. The general  $\lg f_{O_2}$  and temperature range of the upper mantle is from Ref. (21) and Ref. (22), respectively.

Oldhamite is stable when  $\lg f_{\text{O}_2}$  is below the OLS buffer, but cannot exist when  $\lg f_{\text{O}_2}$  is above the OA buffer. At 0.5 GPa and 1320 K,  $\text{OA} = \text{FMQ} + 2.21$  ( $\lg f_{\text{O}_2} = -7.83$ ) and  $\text{OLS} = \text{FMQ} - 0.52$  ( $\lg f_{\text{O}_2} = -10.57$ ) (Fig. 1). The  $\lg f_{\text{O}_2}$  values of Mercury's surface magma range from  $\text{IW} - 2.93$  to  $-10.5$  ( $\lg f_{\text{O}_2} = -13.2$  to  $-21.7$ ) at 1600–1700 K (Fig. 1), and the  $\lg f_{\text{O}_2}$  value of Mercury's atmosphere is  $-14.7$ . These values are much below the OLS buffer (Fig. 1), and no  $\text{H}_2\text{O}$  has been detected in Mercury's atmosphere or at the surface, permitting conservation of oldhamite. On passing, oldhamite indicates an extremely water-deficient and anoxic environment if it is present in large quantities on the surface of a planet, which is unsuitable for most known organisms to survive. On the other side, as a result of high  $\lg f_{\text{O}_2}$  value of  $-4.32$  of the Martian atmosphere and presence of  $\text{H}_2\text{O}$ , no oldhamite but some sulfates have been found on Mars, despite the  $\lg f_{\text{O}_2}$  of Martian magma is actually lower than OLS (Fig. 1). Interestingly, Earth takes an intermediate position between these two cases (though closer to Mars). The average  $\lg f_{\text{O}_2}$  values for arc basalts ( $\text{FMQ} + 0.96$ ), ocean island magma ( $\text{FMQ} + 0.82$ ), and most basalt related to mantle plume on Earth ( $\text{FMQ} + 0.1$ ) are higher than OLS (23). Moreover, the  $\lg f_{\text{O}_2}$  value of  $-0.67$  of Earth's atmosphere is much higher than OA (Fig. 1), and  $\text{H}_2\text{O}$  is abundant in the Earth's crust. The habitable surface conditions for life on Earth do not support the formation of oldhamite. However, most of the oxygen fugacities of the upper mantle are located in the oldhamite stable field (Fig. 1). There must be an interface where  $\text{CaS}$  is converted to  $\text{CaSO}_4$  between the upper mantle and the surface.

Anhydrite has been reported as inclusion in diamonds (24). Reduction of carbonate to diamond/graphite and oxidation of CaS to CaSO<sub>4</sub> are plausibly correlated processes in these cases but the reported paragenesis of anhydrite plus coesite does not provide constraints on the detailed mechanism of formation and entrapment.

In the mantle underneath mid-ocean ridges, at a depth of about 160–170 km, diamond is expected to convert into graphite at an oxygen fugacity above FMQ–2 (25, 26). Redox melting [C (graphite) + 2Fe<sub>2</sub>O<sub>3</sub> (melt) + O<sup>2-</sup> (melt) = 4FeO + CO<sub>3</sub><sup>2-</sup> (both in the melt)] takes place at a depth of around 120–150 km with an oxygen fugacity about FMQ–1.6 (26). The carbonate melt produced by the redox melting will ascend as a flux into the overlying mantle (27). With the decrease of the depth, the oxygen fugacity of mantle gradually increased. At the shallow part, MORBs is characterized by a redox state of FMQ–0.41±0.43 (28), which is closed to FMQ–0.52, the upper limit oxygen fugacity for the stable existence of oldhamite. Thus, the interface where CaS is converted to CaSO<sub>4</sub> exists near or at the solidified MORBs.

There is a large amount of anhydrite and gypsum in the mid-ocean ridges black smoker system. The δ<sup>34</sup>S<sub>V-CDT</sub> value of anhydrite gradually decreases from the seawater's value of 20±1 to 3.4‰, as observed in the 1.8 km deep drillhole in an middle-ocean ridge (29). The δ<sup>34</sup>S<sub>V-CDT</sub> value of 3.4‰, which is much lower than that of modern seawater, is considered to have resulted from the oxidation of low-δ<sup>34</sup>S sulfide to sulfate in the MORB (30). Oldhamite is easily oxidized due to the large negative ΔH<sub>298K</sub> value for Equations 3–5. Thus, the transformation from CaS to CaSO<sub>4</sub> could be a viable route for the formation of sulfate. At 1543 K, the melt temperature

of MORB, the sulfur and calcium isotopic fractionation between anhydrite and oldhamite are  $\delta^{34}\text{S}_{\text{V-CDT}}^{\text{Anh}} - \delta^{34}\text{S}_{\text{V-CDT}}^{\text{Od}} = 10.21\text{‰}$  and  $\delta^{44/40}\text{Ca}^{\text{Anh}} - \delta^{44/40}\text{Ca}^{\text{Od}} = 0.18\text{‰}$ , respectively (Section 6 in the supplementary text). On the contrary, at the same temperature, the sulfur fractionation between sulfate and pyrite, the most abundant sulfide in MORB, is  $\delta^{34}\text{S}_{\text{V-CDT}}^{\text{Sulfate}} - \delta^{34}\text{S}_{\text{V-CDT}}^{\text{Pyrite}} = 3.19\text{‰}$  (31). However, the lowest sulfur isotope of anhydrite 3.4‰ is 5.2 ‰ higher than the mantle sulfur isotope (i.e.,  $\delta^{34}\text{S}_{\text{V-CDT}} = -1.80\text{‰}$  (32)), calling for the role of oldhamite due to relatively large sulfur isotopic fractionation between  $\text{CaSO}_4$  and  $\text{CaS}$ . On the other hand, oldhamite is more easily enriched in light Ca isotopes than the other Ca-bearing minerals (33, 34). The dissolution of  $\text{CaSO}_4$  that have experienced the  $\text{CaS-CaSO}_4$  isotopic fractionation into hydrothermal fluids at the mid-ocean ridges is expected to increase the  $\delta^{44/40}\text{Ca}$  value of hydrothermal fluids relative to the host-rocks, which, indeed, is observed (35). At least part of the anhydrite or gypsum at the middle ocean ridges is a result of the oxidation of  $\text{CaS}$ , which therefore acts as a medium for the C-O-S-Ca cycles in Earth. The hidden oldhamite offers a viable alternative for the origin of sulfate on the Earth and other planets.

## References and notes

1. H. Davy, XXIII. Electro-chemical researches, on the decomposition of the earths; with observations on the metals obtained from the alkaline earths, and on the amalgam procured from ammonia. *Philos. Trans. R. Soc. London* **98**, 333-370 (1808).

2. V. Nasedkin, R. Boyarskaya, Minerals in volcanic-glass pores. *Int. Geol. Rev.* **24**, 1101-1108 (1982).
3. Y. Yanev, A. Benderev, N. Zotov, E. Dubinina, T. Iliev, S. Georgiev, I. Ilieva, I. Sergeeva, Exotic rock block from the Koshava gypsum mine, Northwest Bulgaria: Petrography, geochemistry, mineralogy and melting phenomena. *Geol. Balc.* **50**, 45-65 (2021).
4. C. J. Bennett, J. L. McLain, M. Sarantos, R. D. Gann, A. DeSimone, T. M. Orlando, Investigating potential sources of Mercury's exospheric calcium: photon-stimulated desorption of calcium sulfide. *J. Geophys. Res.: Planets* **121**, 137-146 (2016).
5. C. Defouilloy, P. Cartigny, N. Assayag, F. Moynier, J. A. Barrat, High-precision sulfur isotope composition of enstatite meteorites and implications of the formation and evolution of their parent bodies. *Geochim. Cosmochim. Acta* **172**, 393-409 (2016).
6. R. Brett, M. Sato, Intrinsic oxygen fugacity measurements on seven chondrites, a pallasite, and a tektite and the redox state of meteorite parent bodies. *Geochim. Cosmochim. Acta* **48**, 111-120 (1984).
7. K. Yokoyama, Y. Kimura, C. Kaito, Experiments on condensation of calcium sulfide grains to demarcate environments for the formation of enstatite chondrites. *ACS Earth Space Chem.* **1**, 601-607 (2017).

8. M. M. Wheelock, K. Keil, C. Floss, G. Taylor, G. Crozaz, REE geochemistry of oldhamite-dominated clasts from the Norton County aubrite: Igneous origin of oldhamite. *Geochim. Cosmochim. Acta* **58**, 449-458 (1994).
9. A. V. Sobolev, A. W. Hofmann, S. V. Sobolev, I. K. Nikogosian, An olivine-free mantle source of Hawaiian shield basalts. *Nature* **434**, 590 (2005).
10. S. Lambart, D. Laporte, P. Schiano, An experimental study of pyroxenite partial melts at 1 and 1.5 GPa: Implications for the major-element composition of Mid-Ocean Ridge Basalts. *Earth Planet. Sci. Lett.* **288**, 335-347 (2009).
11. C. Li, E. M. Ripley, The giant Jinchuan Ni-Cu-(PGE) deposit; tectonic setting, magma evolution, ore genesis, and exploration implications. *Rev. Econ. Geol.* **17**, 163-180 (2011).
12. E. Médard, C. A. Mccammon, J. A. Barr, T. L. Grove, Oxygen fugacity, temperature reproducibility, and H<sub>2</sub>O contents of nominally anhydrous piston-cylinder experiments using graphite capsules. *Am. Mineral.* **93**, 1838-1844 (2008).
13. C. W. Haberle, L. A. Garvie, Extraterrestrial formation of oldhamite and portlandite through thermal metamorphism of calcite in the Sutter's Mill carbonaceous chondrite. *Am. Mineral.* **102**, 2415-2421 (2017).
14. R. A. Robie, B. S. Hemingway, Thermodynamic properties of minerals and related substances at 298.15 K and 1 bar (10<sup>5</sup> Pascals) pressure and at higher temperatures. (US Government Printing Office, ed. U.S. Geological Survey Bulletin, 1995).

15. H. S. O'Neill, Free energies of formation of NiO, CoO, Ni<sub>2</sub>SiO<sub>4</sub>, and Co<sub>2</sub>SiO<sub>4</sub>. *Am. Mineral.* **72**, 280-291 (1987).
16. H. S. O'Neill, Quartz-fayalite-iron and quartz-fayalite-magnetite equilibria and the free energy of formation of fayalite (Fe<sub>2</sub>SiO<sub>4</sub>) and magnetite (Fe<sub>3</sub>O<sub>4</sub>). *Am. Mineral.* **72**, 67-75 (1987).
17. M. Keith, K. M. Haase, U. Schwarz-Schampera, R. Klemm, S. Petersen, W. Bach, Effects of temperature, sulfur, and oxygen fugacity on the composition of sphalerite from submarine hydrothermal vents. *Geology* **42**, 699-702 (2014).
18. A. N. Krot, B. Fegley Jr, K. Lodders, H. Palme, Meteoritical and astrophysical constraints on the oxidation state of the solar nebula. *Protostars Planets IV* **1019**, 1019-1054 (2000).
19. C. D. Herd, L. E. Borg, J. H. Jones, J. J. Papike, Oxygen fugacity and geochemical variations in the Martian basalts: Implications for Martian basalt petrogenesis and the oxidation state of the upper mantle of Mars. *Geochim. Cosmochim. Acta* **66**, 2025-2036 (2002).
20. M. Y. Zolotov, A. L. Sprague, S. A. Hauck, L. R. Nittler, S. C. Solomon, S. Z. Weider, The redox state, FeO content, and origin of sulfur-rich magmas on Mercury. *J. Geophys. Res.: Planets* **118**, 138-146 (2013).
21. D. J. Frost, C. A. McCammon, The redox state of Earth's mantle. *Annu. Rev. Earth Planet. Sci.* **36**, 389-420 (2008).

22. U. H. Faul, I. Jackson, The seismological signature of temperature and grain size variations in the upper mantle. *Earth Planet. Sci. Lett.* **234**, 119-134 (2005).
23. E. Cottrell, S. K. Birner, M. Brounce, F. A. Davis, L. E. Waters, K. A. Kelley, Oxygen fugacity across tectonic settings. in *Magma Redox Geochemistry* (Wiley, Hoboken, 2021), pp. 33-61
24. R. Wirth, F. Kaminsky, S. Matsyuk, A. Schreiber, Unusual micro- and nano-inclusions in diamonds from the Juina Area, Brazil. *Earth Planet. Sci. Lett.* **286**, 292-303 (2009).
25. V. Stagno, D. J. Frost, Carbon speciation in the asthenosphere: Experimental measurements of the redox conditions at which carbonate-bearing melts coexist with graphite or diamond in peridotite assemblages. *Earth Planet. Sci. Lett.* **300**, 72-84 (2010).
26. V. Stagno, D. O. Ojwang, C. A. McCammon, D. J. Frost, The oxidation state of the mantle and the extraction of carbon from Earth's interior. *Nature* **493**, 84-88 (2013).
27. R. Dasgupta, M. M. Hirschmann, The deep carbon cycle and melting in Earth's interior. *Earth Planet. Sci. Lett.* **298**, 1-13 (2010).
28. A. Bézoz, E. Humler, The  $\text{Fe}^{3+}/\Sigma\text{Fe}$  ratios of MORB glasses and their implications for mantle melting. *Geochim. Cosmochim. Acta* **69**, 711-725 (2005).

29. D. A. Teagle, J. C. Alt, A. N. Halliday, Tracing the chemical evolution of fluids during hydrothermal recharge: Constraints from anhydrite recovered in ODP Hole 504B. *Earth Planet. Sci. Lett.* **155**, 167-182 (1998).
30. J. C. Alt, E. Zuleger, J. Erzinger, Mineralogy and stable isotopic compositions of the hydrothermally altered lower sheeted dike complex, Hole 504B, Leg 140. in *Proceedings of the Ocean Drilling Program, Scientific Results*. (Citeseer, 1995), pp. 155-166.
31. H. Ohmoto, Isotopes of sulfur and carbon. in *Geochemistry of hydrothermal ore deposits*. (John Wiley & Sons, 1979), pp. 509-567.
32. J. Labidi, P. Cartigny, M. Moreira, Non-chondritic sulphur isotope composition of the terrestrial mantle. *Nature* **501**, 208-211 (2013).
33. F. Huang, C. Zhou, W. Wang, J. Kang, Z. Wu, First-principles calculations of equilibrium Ca isotope fractionation: Implications for oldhamite formation and evolution of lunar magma ocean. *Earth Planet. Sci. Lett.* **510**, 153-160 (2019).
34. C. Zhou, Theoretical calculations of the equilibrium Ca isotope fractionation factors, thesis, University of Science and Technology of China (2019).
35. M. Amini, A. Eisenhauer, F. Böhm, J. Fietzke, W. Bach, D. Garbe-Schönberg, M. Rosner, B. Bock, K. S. Lackschewitz, F. Hauff, Calcium isotope ( $\delta^{44/40}\text{Ca}$ ) fractionation along hydrothermal pathways, Logatchev field (Mid-Atlantic Ridge, 14°45'N). *Geochim. Cosmochim. Acta* **72**, 4107-4122 (2008).

36. X. Zhou, D. He, S. Wang, H. Wang, J. Zhang, Y. Zhao, New exploration on phase transition and structure of PbS under high pressure and temperature. *J. Appl. Phys.* **113**, 043509 (2013).
37. F. Bundy, Phase diagram of Bismuth to 130 000 kg/cm<sup>2</sup>, 500°C. *Phys. Rev.* **110**, 314-318 (1958).
38. K. Aoki, S. Fujiwara, M. Kusakabe, Stability of the bcc structure of bismuth at high pressure. *J. Phys. Soc. Jpn.* **51**, 3826-3830 (1982).
39. K. Bose, J. Ganguly, Quartz-coesite transition revisited: Reversed experimental determination at 500-1200°C and retrieved thermochemical properties. *Am. Mineral.* **80**, 231-238 (1995).
40. S. Ono, T. Kikegawa, Y. Higo, In situ observation of a garnet/perovskite transition in CaGeO<sub>3</sub>. *Phys. Chem. Miner.* **38**, 735-740 (2011).
41. V. Swamy, S. K. Saxena, B. Sundman, J. Zhang, A thermodynamic assessment of silica phase diagram. *J. Geophys. Res.: Solid Earth* **99**, 11787-11794 (1994).
42. M. H. Carr, The fluvial history of Mars. *Philos. Trans. R. Soc., A* **370**, 2193-2215 (2012).
43. A. L. Broadfoot, S. Kumar, M. Belton, M. B. Mcelroy, Mercury's Atmosphere from Mariner 10: Preliminary Results. *Science* **185**, 166-169 (1974).
44. M. Petaev, I. Khodakovsky, Thermodynamic properties and conditions of formation of minerals in enstatite meteorite. in *Chemistry and Physics of Terrestrial Planets*. (Springer, 1986), pp. 106-135.

45. J. Bigeleisen, M. G. Mayer, Calculation of equilibrium constants for isotopic exchange reactions. *J. Chem. Phys.* **15**, 261-267 (1947).
46. Q. Liu, J. A. Tossell, Y. Liu, On the proper use of the Bigeleisen–Mayer equation and corrections to it in the calculation of isotopic fractionation equilibrium constants. *Geochim. Cosmochim. Acta* **74**, 6965-6983 (2010).
47. C. Avril, V. Malavergne, R. Caracas, B. Zanda, B. Reynard, E. Charon, E. Bobocioiu, F. Brunet, S. Borensztajn, S. Pont, Raman spectroscopic properties and Raman identification of CaS-MgS-MnS-FeS-Cr<sub>2</sub>FeS<sub>4</sub> sulfides in meteorites and reduced sulfur-rich systems. *Meteorit. Planet. Sci.* **48**, 1415-1426 (2013).
48. P. Makreski, G. Jovanovski, S. Dimitrovska, Minerals from Macedonia: XIV. Identification of some sulfate minerals by vibrational (infrared and Raman) spectroscopy. *Vib. Spectrosc.* **39**, 229-239 (2005).
49. J. L. Morton, N. H. Sleep, A mid-ocean ridge thermal model: Constraints on the volume of axial hydrothermal heat flux. *J. Geophys. Res.: Solid Earth* **90**, 11345-11353 (1985).

### **Acknowledgements**

We are very grateful to Professor D.L. Khoshtedt, Professor H.F. Zhang, Professor Y.S. Liu, and Professor S.C. Huang for the great help in improving this manuscript and constructive comments. **Funding:** I.M.C. and S.H.M. thank the financial support of Chinese Academy of Sciences (Grant No. QYZDY-SSW-DQC008 to I.M.C. and

Grants No. QYZDY-SSW-DQC029 and No. XDA22040501 to S.H.M.). L.P.W acknowledges support from the Major Science and Technology Infrastructure Project of Material Genome Big-science Facilities Platform supported by Municipal Development and Reform Commission of Shenzhen. Y.G.L. is grateful to the financial support by State Scholarship Fund ([2016]3035-201608610016) from the China Scholarship Council. **Author contributions:** Y.G.L., S.H.M., and L.P.W. conceived and designed the study. Y.G.L. wrote the manuscript. I.M.C, J.Z.C, and Y.G.L calculated the OA and OLS buffers. N.P.W, J.Z.C, and Y.G.L calculated the sulfur isotopic fractionation factor. All authors conducted the analyses and contributed to interpreting the data. **Competing interests:** The authors declare no competing interests. **Data and materials availability:** All data are available in the supplementary materials.